

UCSF

UC San Francisco Previously Published Works

Title

Technical Note: Evaluation of audiovisual biofeedback smartphone application for respiratory monitoring in radiation oncology

Permalink

<https://escholarship.org/uc/item/4jn9j53j>

Journal

Medical Physics, 47(11)

ISSN

0094-2405

Authors

Capaldi, Dante PI
Nano, Tomi F
Zhang, Hao
[et al.](#)

Publication Date

2020-11-01

DOI

10.1002/mp.14484

Peer reviewed



Published in final edited form as:

Med Phys. 2020 November ; 47(11): 5496–5504. doi:10.1002/mp.14484.

Technical Note: Evaluation of Audiovisual Biofeedback Smartphone Application for Respiratory Monitoring in Radiation Oncology

Dante P.I. Capaldi, PhD¹, Tomi F. Nano, PhD², Hao Zhang, PhD¹, Lawrie B. Skinner, PhD¹, Lei Xing, PhD¹

¹Department of Radiation Oncology, School of Medicine, Stanford University, Stanford, California, USA

²University of California, San Francisco (UCSF) Comprehensive Cancer Centre, San Francisco, California, USA

Abstract

Purpose—Radiation dose delivered to targets located near the upper abdomen or thorax are significantly affected by respiratory motion, necessitating large margins, limiting dose escalation. Surrogate motion management devices, such as the Real-time Position Management (RPM™) system (Varian Medical Systems, Palo Alto, CA), are commonly used to improve normal tissue sparing. Alternative to current solutions, we have developed and evaluated the feasibility of a real-time position management system that leverages the motion data from the onboard hardware of Apple iOS devices to provide patients with visual coaching with the potential to improve the reproducibility of breathing as well as improve patient compliance and reduce treatment delivery time.

Methods and Materials—The iOS application, coined the *Instant Respiratory Feedback* (IRF) system, was developed in Swift (Apple Inc., Cupertino, CA) using the Core-Motion library and implemented on an Apple iPhone® devices. Operation requires an iPhone®, a 3D printed arm, and a radiolucent projector screen system for feedback. Direct comparison between IRF, which leverages sensor fusion data from the iPhone®, and RPM™, an optical based system, was performed on multiple respiratory motion phantoms and volunteers. The IRF system and RPM™ camera tracking marker were placed on the same location allowing for simultaneous data acquisition. The IRF surrogate measurement of displacement was compared to the signal trace acquired using RPM™ with univariate linear regressions and Bland-Altman analysis.

Results—Periodic motion shows excellent agreement between both systems, and subject motion shows good agreement during regular and irregular breathing motion. Comparison of IRF and RPM™ show very similar signal traces that were significantly related across all phantoms, including those motion with different amplitude and frequency, and subjects' waveforms (all $r > 0.9$, $p < 0.0001$). We demonstrate the feasibility of four-dimensional cone beam computed

Correspondence to: L. Xing PhD, Department of Radiation Oncology, School of Medicine, Stanford University, 875 Blake Wilbur Dr, Stanford, California, USA, 94305, lei@stanford.edu.

Conflict of Interest: None.

tomography reconstruction using IRF can acquire dynamic phantom images with similar image quality as RPM™.

Conclusions—Feasibility of an iOS application to provide real-time respiratory motion is demonstrated. This system generated comparable signal traces to a commercially available system and offers an alternative method to monitor respiratory motion.

Keywords

RPM; Motion Management; Apple iOS Application; Smartphone; Accelerometer; Gyroscope; Sensor Fusion; Respiratory Motion; 4D CBCT

1. INTRODUCTION

Radiation dose delivered to a target located near the upper abdomen or thorax is significantly affected by respiratory motion stemming from the expansion and contraction of diaphragmatic and intercoastal muscles. Relatively large margins are commonly added to the Clinical Target Volume (CTV) to compensate for this motion - limiting dose escalation capability.^{1, 2} Accordingly, breath-hold or respiratory gating radiotherapy has been implemented to reduce margins and dose escalate,³⁻⁵ which has been leveraged to facilitate sophisticated techniques such as stereotactic ablative radiotherapy or stereotactic body radiation therapy (SABR/SBRT).^{2, 6} The efficacy of these methods is largely determined by the patient's ability to breathe consistently, where previous studies have reported large inter- and intra-variability.^{5, 7, 8} To improve the reproducibility of these methods, audiovisual feedback systems have been previously developed and shown to improve lung tumor position reproducibility and volume consistency.^{9, 10}

Paramount to the implementation of gating or breath-hold radiotherapy is the detection of respiratory signals using either internal or external probes to track and monitor respiratory motion.¹¹ Both internal and external surrogates of tumor motion are currently being used in the clinic as respiratory monitors. Internal surrogates of target motion consist of implanting a fiducial marker in the vicinity of the tumor either to be track using fluoroscopy or radiofrequency waves with radiopaque markers or Calypso® (Varian Medical Systems, Palo Alto, CA) beacon transponders, respectively. Internal fiducials provide real-time motion of the tumor, albeit invasive procedures are required for implantation. Real-time tracking using cine-imaging methods have also been proposed to track tumor motion and gate the radiation beam using systems such as the "MR-linac" - a magnetic resonance imaging (MRI) machine and a linear accelerator combined into a single device - but are currently limited to a few clinics. Alternatively, external surrogates of tumor motion have been proposed to provide a non-invasive solution to monitor respiratory motion. Many different methods have been investigated to acquire external respiratory signals, including optical systems such as the Microsoft Kinect that measures displacement of surfaces or spirometers to measure lung volumes, as well as to Calypso® (Varian Medical Systems) that can also be used for surface motion tracking using surface transponders.¹¹ One common commercial system is the Real-time Position Management (RPM™) system by Varian (Varian Medical Systems), which makes use of an infrared camera and a reflective marker box that is placed on a patients' abdomen to provide continuous motion tracking.

Alternative methods with lower costs have been proposed, specifically using accelerometer-based methods^{12, 13} which are widely accessible with the ubiquity of smartphones. Unfortunately, motion detected using only accelerometers has low signal-to-noise and causes signal drift, requiring fine-tuned signal processing techniques to acquire smooth respiratory waveforms to minimize the effects due numerical integration error in deriving displacement from acceleration.^{12, 13} With recent advances, these issues have been minimized with the incorporation of sensor fusion,¹⁴ which reduces drift and uncertainty in angular orientation measurement via integration of multiple sensors (i.e. acceleration and gyroscopic information commonly acquired on smartphone devices). In the present work, a real-time position monitoring system, coined the *Instant Respiratory Feedback (IRF)* system, that leverages accurate motion related data from onboard hardware in Apple iOS devices is developed and evaluated. The IRF system was also integrated into a current clinical audiovisual-assisted therapeutic ambience in radiation therapy (AVATAR) system^{15, 16} and evaluated its ability to measure surface motion by comparing it to a commercial system.

2. MATERIALS AND METHODS

2.1. Development of the iOS Application

In this study, an Apple iOS application (Apple Inc., Cupertino, CA) was developed in Xcode, Apple's integrated development environment (IDE), using the Swift programming language, available from the authors online (<https://github.com/capalddid/IRF>). The interface of the application, as shown in Figure 1A, has three main functions: 1) the "Reference" metronome signal, 2) patient specific respiratory trace, and 3) save/record. The metronome was integrated into the design of the application in an effort to assist in coaching prospective patients to perform periodic breathing, which has been shown to be advantageous for radiotherapy treatment gating,¹⁷ and four dimensional (4D) imaging procedures, such as 4D cone beam computed tomography (4D CBCT) acquisitions. The respiratory trace is the real-time trace of the patients' movement. The trace can be recorded and saved, as shown in the online supplementary video, and the data (both time and signal) is sent wirelessly in a comma separated value (CSV) file. The motion data is acquired using the Core Motion framework, at a sampling frequency of 10 Hz, which incorporates sensor fusion to improve motion data. For simplicity, the user is given an indication from 0 to 100, representing the minimum and maximum displacement, to assist in the coaching of patients breathing maneuvers.

2.2. Implementation of IRF

The signal that is acquired from the Apple iPhone® (Apple Inc.) was the pitch of the phone, as shown in Figure 1B, with an accuracy of $\pm 0.1^\circ$. The iPhone® is placed on a 3D printed arm that was designed in Autodesk Fusion 360 (Autodesk, San Rafael, CA) and printed using an Ultimaker S5 three-dimensional (3D) printer (Ultimaker, Cambridge, MA), illustrated in Figure 1C. The design is available from the authors online (<https://github.com/capalddid/IRF>). The arm was designed to have the ability to rotate as well as translate about a point (indicated by the red bounding box), facilitating an accurate calculation of displacement in the anterior-posterior direction as the point of contact can be held constant (where the arm is affixed to the patient surface – illustrated as the black foot in Figure 1C).

For our experiments, the foot of the IRF arm was taped in place as to prevent it from moving. Knowing the length of the adjacent side of the triangle is constant (l), and the pitch is measured continuously (θ), the displacement (d) can be calculated using the following equation:

$$d = l \times \tan\theta \quad (1)$$

In addition, the iPhone® was connected to a preexisting clinical radiolucent audio-visual (AVATAR) system,^{15, 16} shown in Figure 1D (phantom) and Figures 1E & 1F (volunteer). The cephalad AVATAR system mounts a portable projector to the head of the treatment table, displaying a video on a screen, which was used to display the application from the iPhone® for the patient to visualize while performing coached breathing.

2.3. Evaluating the Accuracy of IRF

The accuracy of the proposed IRF system was evaluated on two motion phantoms and two volunteers – subjected to a variety of respiratory motion waveforms. The motion phantoms that were used in this study was the Respiratory Position Management phantom (Varian Medical Systems) as well as the Dynamic Thorax Motion Phantom (CIRS, Norfolk, VA). The latter phantom was used to program respiratory waveforms with varying amplitude and period. The iPhone® and RPM™ marker box were located in the same location allowing for simultaneous data acquisition on a Varian Clinac 21X (Varian Medical Systems) to evaluate the accuracy of measuring displacement. Drift was evaluated by averaging the amplitude in the first half and comparing it with the second half of a stationary generated waveform acquired simultaneously with both systems. For the volunteers, the AVATAR screen was used to instruct breathing maneuvers – one volunteer was instructed to breathe normally (in addition to taking a deep-breath) while the other volunteer was requested to perform irregular breathing maneuvers, such as coughing and panting, specifically to mimic patient conditions. Both the RPM™ and IRF respiratory traces were acquired and halted simultaneously, where the end location of the trace was used as the starting location to perform comparisons.

Additionally, to demonstrate an alternative application of the IRF system, the Dynamic Thorax Motion Phantom (CIRS) was placed on a Varian TrueBeam (Varian Medical Systems) capable of acquiring 4D CBCT. Both the IRF and RPM™ marker box were placed at the same location on the phantom to simultaneously acquire respiratory trace data while imaging the phantom in motion using a half-fan CBCT protocol for the thorax. Raw half-fan projection CBCT data was exported and reconstructed in MATLAB R2019a (Mathworks, Natick, Massachusetts, USA) and corrected for displacement in the detector.¹⁸ 4D CBCT reconstruction was performed by binning the raw projections based on their respective respiratory phase information provided by either RPM™ or IRF and reconstructed using a simple the Feldkamp, Davis, Kress (FDK) filtered back-projection algorithm.

2.4. Statistics

Shapiro-Wilk tests were used to determine the normality of the data. In order to quantitatively evaluate the accuracy, the absolute means and standard deviation for the

displacement (maximum, average, and minimum) and the period were calculated. Relationships between displacement measurements acquired using the RPM™ and the proposed IRF systems were determined using Pearson coefficients (r).¹⁹ The Bland–Altman method was used to evaluate measurement agreement.²⁰ Results were considered significant when the probability of two-tailed type I error (α) was less than 5% ($p < .05$). Statistical analysis was performed using GraphPad Prism V8.1.2 (GraphPad Software Inc., La Jolla, CA).

3. RESULTS

Figure 2 illustrates the comparison of the signal traces acquired simultaneously between the RPM™ system (Varian Medical Systems) and the developed IRF iOS application. Displacement measured using both systems showed excellent agreement for the RPM phantom as well as both volunteers – one of which performed irregular breathing maneuvers, specifically coughing and panting, to simulate similar scenarios as a patient with lung disease. Furthermore, there was no observation of signal drift common amongst accelerometer-based methods that measure displacement.

Figure 2 shows comparison of the signal traces acquired simultaneously with the RPM™ system (Varian Medical Systems) and the developed IRF iOS application using the Dynamic Thorax Motion Phantom (CIRS). The phantom was programmed to generate motion waveforms at different amplitudes (Low = 1 cm, Medium = 1.5 cm, High = 2 cm) and frequencies (Low = 0.1 Hz, Medium = 0.2 Hz, High = 4 Hz). Excellent agreement in measured displacement was observed across the range waveforms produced by the motion phantom. The absolute differences in amplitude (absolute maximum, mean, and minimum peak) and period between the IRF and RPM™ systems are listed in Table 1.

Figure 3 shows the relationships between the IRF and the RPM™ systems for the RPM phantom as well as both volunteers. IRF was significantly correlated with RPM™ having unity-slope for: the RPM phantom ($r = 0.997$, $r^2 = 0.994$, $p < 0.0001$, slope = 0.939), the one volunteer that was instructed to breathe normally and take a deep breath in ($r = 0.996$, $r^2 = 0.991$, $p < 0.0001$, slope = 0.962), as well as the other volunteer who performed irregular breathing simulating patients with respiratory disease ($r = 0.981$, $r^2 = 0.962$, $p < 0.0001$, slope = 0.918). Bland-Altman analysis of agreement for IRF with RPM™ demonstrated that the RPM phantom (bias = -0.02 ± 0.04 cm, 95% confidence interval = -0.11 cm - 0.06 cm) and both volunteers (volunteer 1: bias = 0.01 ± 0.09 cm, 95% confidence interval = -0.17 cm - 0.18 cm; volunteer 2: bias = 0.07 ± 0.15 cm, 95% confidence interval = -0.22 cm - 0.36 cm) had marginal bias. Table 2 shows the relationships for all different waveforms, including those generated from the CIRS Dynamic Thorax Motion Phantom.

Figure 4 shows 4D CBCT images acquired using the CIRS Dynamic Thorax Motion Phantom and reconstructed using respiratory information provided by the IRF and RPM™ systems. The FDK back-projection algorithm reconstruction using the respiratory phase information provided by either RPM™ or IRF systems provided good qualitative agreement when compared at both inspiration and expiration phases.

4. DISCUSSION

In this study, an Apple iOS application to evaluate motion in real-time was developed and applied to respiratory phantoms as well as volunteers and the following findings were observed: 1) IRF was highly correlated with the RPM™ system; 2) IRF demonstrated accurate quantification of displacement when subjected to a variety of different breathing patterns, including periodic and irregular breathing, and; 3) the iOS application is easily implementable into current clinical workflows- facilitated by the AVATAR system.

The IRF iOS system was compared to RPM™ and both systems were found to produce similar motion traces even though they have different methods of operation. Displacement of periodic motion and irregular breathing were accurately quantified with the IRF system. Sensor-fusion of the iPhone® accelerator and gyroscope signals allows for reliable measurement of angular orientation without the need for drift-correcting signal processing filters. In combination with the IRF arm, angular measurement from the iPhone® is converted to displacement along a single axis. Placement of the IRF lever arm can be used for various patient anatomies, couch-kick positions and gantry rotations as it does not rely on external sensors that could cause occlusion problems.²¹

The IRF AVATAR system displays real-time feedback to the patient, which could be helpful in providing more consistent breathing patterns during treatment, as previously demonstrated with alternative approaches.²² Other motion management systems, such as SDX™ spirometry system (DYN'R Medical Systems, Aix-en-Provence, France), already utilize video guidance to assist patients in performing breath-hold techniques during inspiration and expiration. In addition to breath-hold techniques, the IRF user display has a metronome that provides free-breathing visual feedback in real-time. Providing motion feedback to the patient, which improves breathing motion consistency, could provide further confidence to clinicians for using smaller margins or high dose hypofractionation stereotactic radiation techniques. Additionally, we demonstrated one implementation of the IRF to generate 4D CBCT as a potential application to retrospectively sort CBCT acquired while free breathing to produce phase binned image volumes. Similar to previous studies where multiple external surrogates were simultaneously acquired for 4DCT sorting, they observed slight differences in waveforms which did not translate to changes in image quality.²³

In this proof-of-concept study of the IRF iOS system, we were limited in our system evaluation by the use of two phantoms, measuring breathing traces from two healthy volunteers, and using the RPM™ system as our ground-truth for motion comparison. Other phantoms that incorporate more sophisticated user-specified motion inputs, such as real patient motion that was pre-recorded, could be used in the future for further evaluation. In addition, inter- and intra-patient variation for all motion management systems could be evaluated in terms of their reproducibility and accuracy by using a population of patients and volunteers. By having RPM™ as our motion reference, we were limited by the RPM™ measurement and found cases where there was inconsistency between the reference and our IRF system. This study provides evidence that the IRF iOS system could be further evaluated for motion management in radiation therapy and radiology 4D acquisitions, as

demonstrated in this study using CBCT. Lastly, although this method provides a surrogate to respiratory motion in one-dimension (vertical), other systems, such as Vision RT (Vision RT Ltd, London, United Kingdom) that use optical tracking²⁴ as well as recent versions of RPM™, have the ability to provide motion in the longitudinal and lateral directions as well as rotations. One-dimensional signals, such as the one proposed in our study as well as spirometry, respiratory bellows, and previous versions of RPM™ that are still being used clinically, do not fully describe the complex motion of breathing. Furthermore, any external measurement is only a surrogate of the true motion of the target, while internal markers, such as the Calypso™, or imaging using the MR-linac can provide true target motion. Previous work has demonstrated that single marker-based tracking have the potential to result in geographic inaccuracies, where additional multiple external markers or measurements can assist in detecting errors from breathing motion changes.²⁵ A future direction of this work will be to develop technology that leverages multiple accelerometers on different locations on the body to better describe the motion and assist in detecting errors from breathing motion changes, as previously described.²⁶ Additionally, future studies will focus on the reproducibility of the system on a group of subjects across multiple users and timepoints.

Previous studies have investigated the use of acceleration sensors for respiratory monitoring,^{12, 13} albeit mainly focusing on the challenges associated with accelerometers and how to compensate for the low signal-to-noise, causing signal drift and errors when deriving displacement from acceleration. Furthermore, these studies did not explicitly demonstrate the feasibility of using their systems for audiovisual biofeedback, where the previous work extracted signals retrospectively for analysis. In this study, the issues previously faced with accelerometer technology was overcome by the recent advances in sensor fusion embedded in most smartphones,¹⁴ reducing uncertainty in measurements and facilitating the deployment of accelerometers for respiratory motion monitoring. Additionally, we present an iOS application that has the capability to not only capture motion, but also display (with the use of the AVATAR system) the respiratory traces to the patients as well as a “reference” metronome signal to assist in coaching patients to perform specific breathing maneuvers, which has previously been shown in studies to improve the efficacy of radiotherapy delivery,²⁷ as well as improve the reproducibility of the frequency and amplitude of breathing, improve patient compliance and reduce treatment delivery time.^{28–32} Although our system is not directly connected to the delivery system, audiovisual biofeedback can improve the quality and delivery of radiation as the patient is able to see their trace and ultimately correct for their own breathing - providing the radiation therapists with consistent and more predictable breathing patterns. Furthermore, the potential benefit and convenience of this technology being a smartphone application is that patients could download this application to their phones as a way to assist in patient education and teach patients to practice at home, in an effort to further improve the overall efficacy and experience during treatment. IRF has the potential to be implemented across the clinical workflow - from assisting in acquiring gated imaging used for treatment planning at simulation all the way to the delivery of treatment.

In summary, the IRF system provides a real-time respiratory motion management solution as an alternative to commercially available products and exhibits strong agreement. This iOS

application has the potential to facilitate the translation of respiratory gated techniques to centers that currently do not have access to respiratory motion management systems, in an effort to improve the efficacy of radiation therapy.

Supplementary Material

Refer to Web version on PubMed Central for supplementary material.

Acknowledgements

Dr. Capaldi receives funding support from the Natural Sciences and Engineering Research Council (NSERC) of Canada Postdoctoral Fellowship Program. This work is partially supported by Grants (1R01CA223667 and 1R01CA227713) from the National Institute of Health (NIH/NCI).

5. REFERENCES

- Keall PJ, Mageras GS, Balter JM, et al., The management of respiratory motion in radiation oncology report of AAPM Task Group 76, *Med. Phys* 33(10), 3874–3900 (2006). [PubMed: 17089851]
- Timmerman RD and Xing L, *Image-guided and adaptive radiation therapy* (Lippincott Williams & Wilkins, 2012).
- Ozhasoglu C and Murphy MJ, Issues in respiratory motion compensation during external-beam radiotherapy, *Int. J. Radiat. Oncol. Biol. Phys* 52(5), 1389–1399 (2002). [PubMed: 11955754]
- Vedam SS, Keall PJ, Kini VR, and Mohan R, Determining parameters for respiration-gated radiotherapy, *Med. Phys* 28(10), 2139–2146 (2001). [PubMed: 11695776]
- Xing L, Thorndyke B, Schreiber E, et al., Overview of image-guided radiation therapy, *Med. Dosim* 31(2), 91–112 (2006). [PubMed: 16690451]
- Timmerman R, Paulus R, Galvin J, et al., Stereotactic body radiation therapy for inoperable early stage lung cancer, *JAMA - J. Am. Med. Assoc* 4(9), 1263–1266 (2010).
- Seppenwoolde Y, Shirato H, Kitamura K, et al., Precise and real-time measurement of 3D tumor motion in lung due to breathing and heartbeat, measured during radiotherapy, *Int. J. Radiat. Oncol. Biol. Phys* 53(4), 822–834 (2002). [PubMed: 12095547]
- Bruce EN, Temporal variations in the pattern of breathing, *J. Appl. Physiol* 80(4), 1079–1087 (1996). [PubMed: 8926229]
- Lee D, Greer PB, Lapuz C, et al., Audiovisual biofeedback guided breath-hold improves lung tumor position reproducibility and volume consistency, *Adv. Radiat. Oncol* 2(3), 354–362 (2017). [PubMed: 29114603]
- Park YK, Kim S, Kim H, Kim IH, Lee K, and Ye SJ, Quasi-breath-hold technique using personalized audio-visual biofeedback for respiratory motion management in radiotherapy, *Med. Phys* 38(6), 3114–3124 (2011). [PubMed: 21815385]
- Bertholet J, Knopf A, Eiben B, et al., Real-time intrafraction motion monitoring in external beam radiotherapy, *Phys. Med. Biol* 64(15), 33pp (2019).
- Ono T, Takegawa H, Ageishi T, et al., Respiratory monitoring with an acceleration sensor, *Phys. Med. Biol* 56(19), 6279–6289 (2011). [PubMed: 21896964]
- Capaldi D, Zhang H, Nano T, et al., MO-C930-GePD-F6-05: Tracking Respiratory Motion in Radiation Oncology Without Optical Or Stress Gauge Devices: A Low-Cost Accelerometer Based Real-Time Position Management (RPM) System, in *Med. Phys*(2019), pp. E235–E235.
- Guiry JJ, van de Ven P, and Nelson J, Multi-sensor fusion for enhanced contextual awareness of everyday activities with ubiquitous devices, *Sensors (Switzerland)* 14(3), 5687–5701 (2014).
- Hiniker SM, Bush K, Fowler T, et al., Initial clinical outcomes of audiovisual-assisted therapeutic ambience in radiation therapy (AVATAR), *Pract. Radiat. Oncol* 7(5), 311–318 (2017). [PubMed: 28242188]

16. Balazy KE, Gutkin PM, Skinner L, et al., Impact of Audio-Visual Assisted Therapeutic Ambience in Radiotherapy (AVATAR) on Anesthesia Use, Payer Charges, and Treatment Time in Pediatric Patients, *Pract. Radiat. Oncol* Ahead-of-print (2020).
17. Giraud P and Houle A, Respiratory Gating for Radiotherapy: Main Technical Aspects and Clinical Benefits, *ISRN Pulmonol.* 2013, pp13 (2013).
18. Wang G, X-ray micro-CT with a displaced detector array, *Med. Phys* 29(7), 1634–1636 (2002). [PubMed: 12148746]
19. Lin LI-K, A Concordance Correlation Coefficient to Evaluate Reproducibility, *Biometrics* 45(1), 255–268 (1989). [PubMed: 2720055]
20. Altman DG, *Practical statistics for medical research* (CRC press, 1990).
21. García-Vázquez V, Marinetto E, Santos-Miranda JA, Calvo FA, Desco M, and Pascau J, Feasibility of integrating a multi-camera optical tracking system in intra-operative electron radiation therapy scenarios, *Phys. Med. Biol* 58(24), 8769–8782 (2013). [PubMed: 24301181]
22. Kini VR, Vedam SS, Keall PJ, Patil S, Chen C, and Mohan R, Patient training in respiratory-gated radiotherapy, *Med. Dosim* 28(1), 7–11 (2003). [PubMed: 12747612]
23. Glide-Hurst CK, Smith MS, Ajlouni M, and Chetty IJ, Evaluation of two synchronized external surrogates for 4D CT sorting, *J. Appl. Clin. Med. Phys* 14(6), 117–132 (2013).
24. Gopan O and Wu Q, Evaluation of the accuracy of a 3D surface imaging system for patient setup in head and neck cancer radiotherapy, *Int. J. Radiat. Oncol. Biol. Phys* 84(2), 547–552 (2012). [PubMed: 22365627]
25. Park Y, Son T, Kim H, et al., Development of real-time motion verification system using in-room optical images for respiratory-gated radiotherapy, *J. Appl. Clin. Med. Phys* 14(5), 25–42 (2013). [PubMed: 24036857]
26. Gaidhani A, Moon KS, Ozturk Y, Lee SQ, and Youm W, Extraction and analysis of respiratory motion using wearable inertial sensor system during trunk motion, *Sensors* 17(12), 2932 (2017).
27. Kim A, Kalet AM, Cao N, et al., Effects of Preparatory Coaching and Home Practice for Deep Inspiration Breath Hold on Cardiac Dose for Left Breast Radiation Therapy, *Clin. Oncol* 30(9), 571–577 (2018).
28. Peng Y, Vedam S, Chang JY, et al., Implementation of feedback-guided voluntary breath-hold gating for cone beam CT-based stereotactic body radiotherapy, *Int. J. Radiat. Oncol. Biol. Phys* 80(3), 909–917 (2011). [PubMed: 21470784]
29. Nakamura M, Narita Y, Matsuo Y, et al., Effect of audio coaching on correlation of abdominal displacement with lung tumor motion, *Int. J. Radiat. Oncol. Biol. Phys* 75(2), 558–563 (2009). [PubMed: 19735881]
30. Linthout N, Bral S, Van de Vondel I, et al., Treatment delivery time optimization of respiratory gated radiation therapy by application of audio-visual feedback, *Radiother. Oncol* 91(3), 330–335 (2009). [PubMed: 19368987]
31. Yoshitake T, Nakamura K, Shioyama Y, et al., Breath-hold monitoring and visual feedback for radiotherapy using a charge-coupled device camera and a head-mounted display: system development and feasibility, *Radiat. Med* 26(1), 50–55 (2008). [PubMed: 18236136]
32. Kim T, Pollock S, Lee D, O'Brien R, and Keall P, Audiovisual biofeedback improves diaphragm motion reproducibility in MRI, *Med. Phys* 39(11), 6921–6928 (2012). [PubMed: 23127085]

Novelty & Significance of Study

In this study, we developed and evaluated a real-time position management system that leverages the motion related data from the onboard hardware of Apple iOS devices. We demonstrated the feasibility of this iOS application, coined the *Instant Respiratory Feedback* system, to provide real-time respiratory motion using an audiovisual system and exhibited strong agreement with Varian's Real-time Position Management™ system. The proposed iOS application has the potential to facilitate the translation of respiratory gated techniques, such as deep inspiration breath-holds or four-dimensional cone beam computed tomography, to centers that currently do not have access to respiratory motion management systems, in an effort to improve the efficacy of radiotherapy.

Author Manuscript

Author Manuscript

Author Manuscript

Author Manuscript

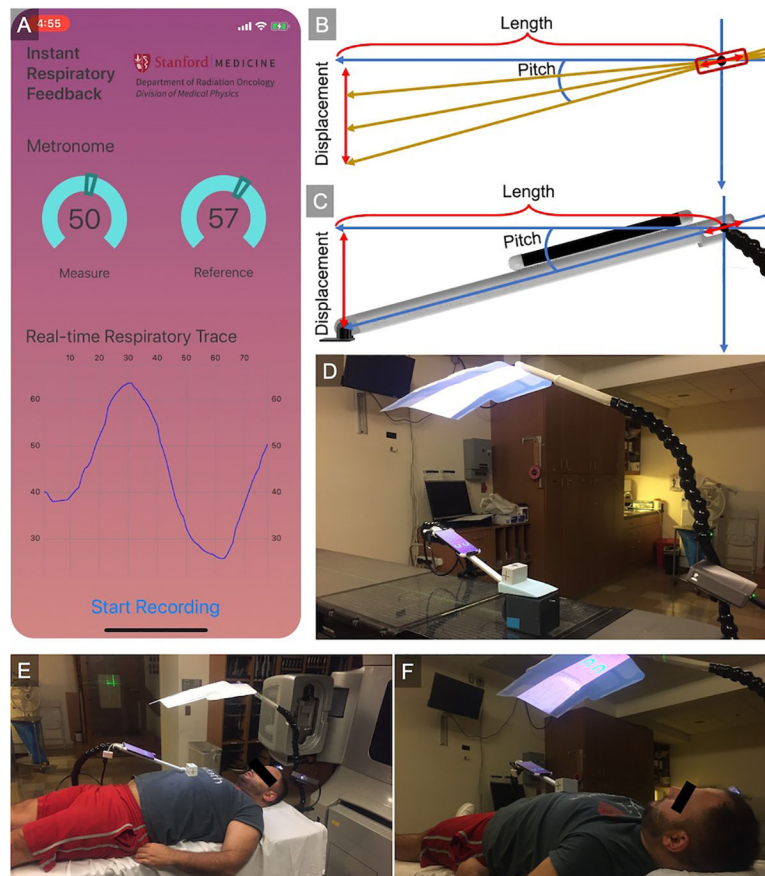


Figure 1. Application and procedure for acquiring displacement from the IRF iOS application. (A) Screen capture of the iOS application showing the Core Motion framework which incorporates sensor fusion to improve motion data (supplementary video illustrating the operation of the application). (B) Schematic of the procedure to acquire the displacement as well as (C) a 3D design of the experimental setup. (D) Experimental layout on a linear accelerator couch with the motion phantom as well as the AVATAR system¹⁵. Experimental setup illustrating (E) placement of the IRF arm used to support the iPhone® away from the treatment field as well as (F) the AVATAR system providing visual feedback of the respiratory trace back to the patient to assist in coaching to perform specific breathing maneuvers (i.e. breath-hold, free-breathing).

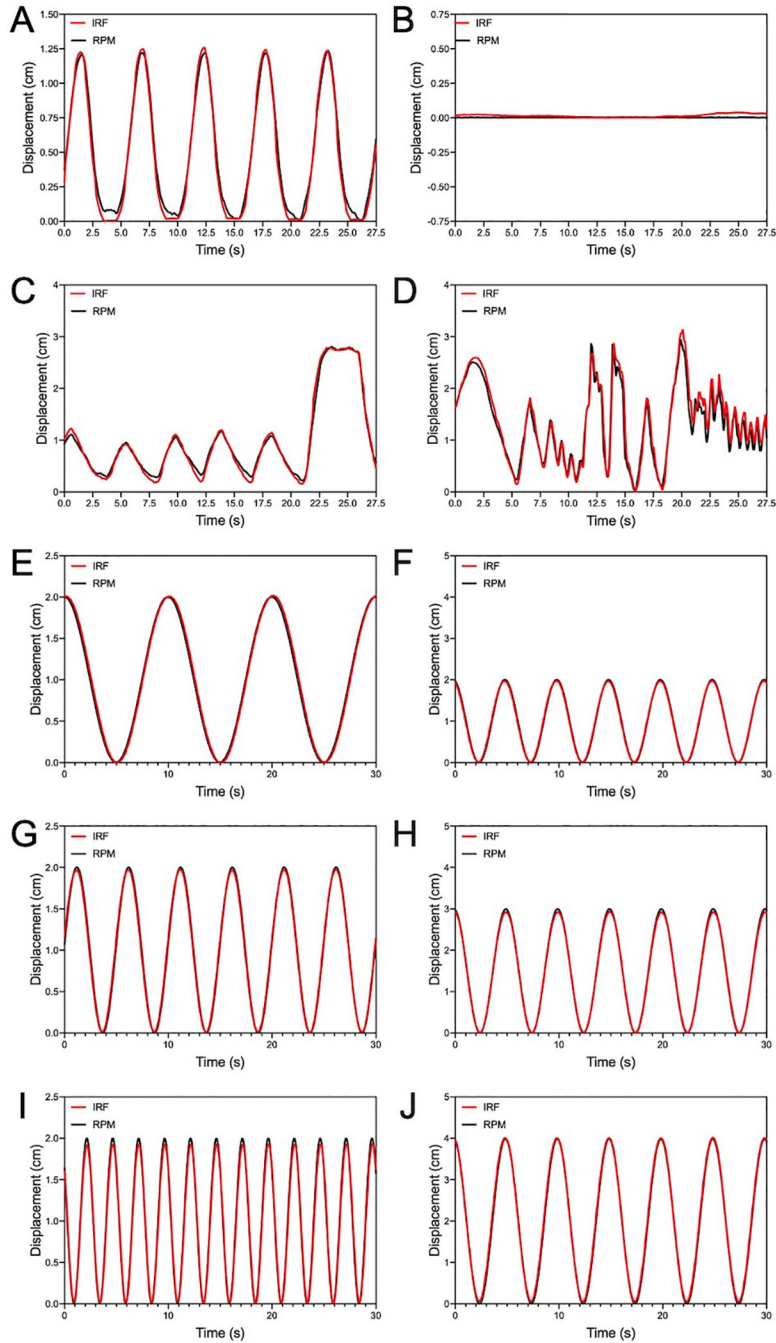


Figure 2. Comparison of the RPM™ system and the IRF iOS application traces of RPM™ phantom (A, B) while in motion and stationary, as well as two volunteers' motion (C, D) and the CIRS Dynamic Thorax Motion Phantom at various waveform settings. Periodic motion measured from the RPM™ phantom and volunteer shows excellent agreement between both systems, and the subject motion shows good agreement of irregular motion. One volunteer was instructed to perform normal breathing in addition to taking a deep breath (C) while the other volunteer was requested to perform irregular breathing maneuvers, specifically

coughing and panting, to simulate similar scenarios as a patient with lung disease (**D**). Variations in both period (**E, G, I**) and amplitude (**F, H, J**) motion programmed using the CIRS Dynamic Thorax Motion Phantom shows excellent agreement between both systems. Red-line = IRF iOS application; black-line = RPM™ system.

Author Manuscript

Author Manuscript

Author Manuscript

Author Manuscript

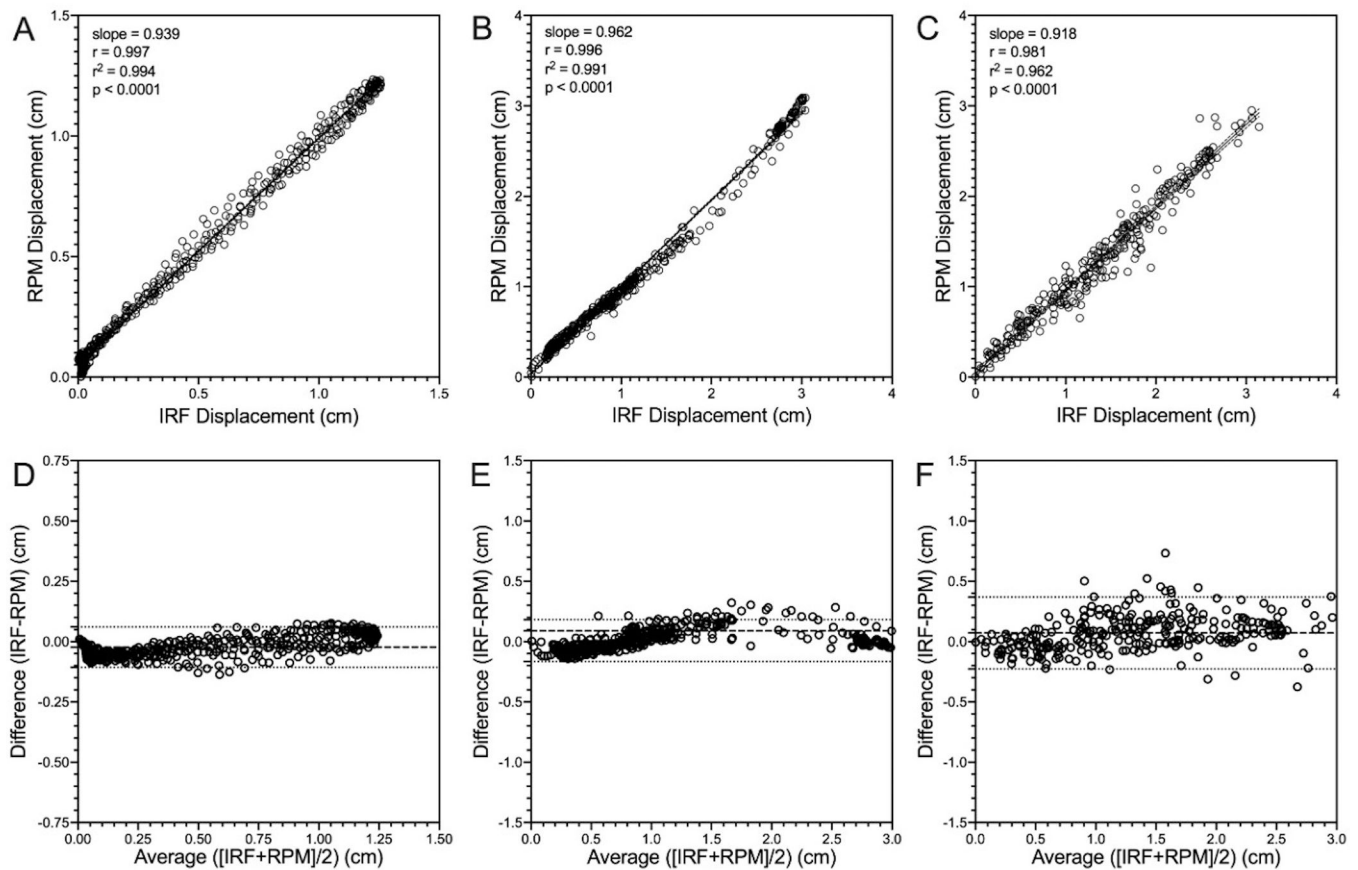


Figure 3.

Relationship between RPM™ system and the IRF iOS application traces acquired from the RPM™ motion phantom and volunteer subjects. IRF was significantly correlated with and RPM™ system [Phantom (A): $r = 0.997$, $r^2 = 0.994$, $p < 0.0001$, slope = 0.939; Volunteer 1 (B): $r = 0.996$, $r^2 = 0.991$, $p < 0.0001$, slope = 0.962; Volunteer 2 (C): $r = 0.981$, $r^2 = 0.962$, $p < 0.0001$, slope = 0.918]. Bland-Altman analysis of agreement for IRF with RPM™ [Phantom (D): bias = -0.02 ± 0.04 cm, lower limit = -0.11 cm, upper limit = 0.06 cm; Volunteer 1 (E): bias = 0.01 ± 0.09 cm, lower limit = -0.17 cm, upper limit = 0.18 cm; Volunteer 2 (F): bias = 0.07 ± 0.15 cm, lower limit = -0.22 cm, upper limit = 0.36 cm). Dotted lines indicate the 95% confidence interval.

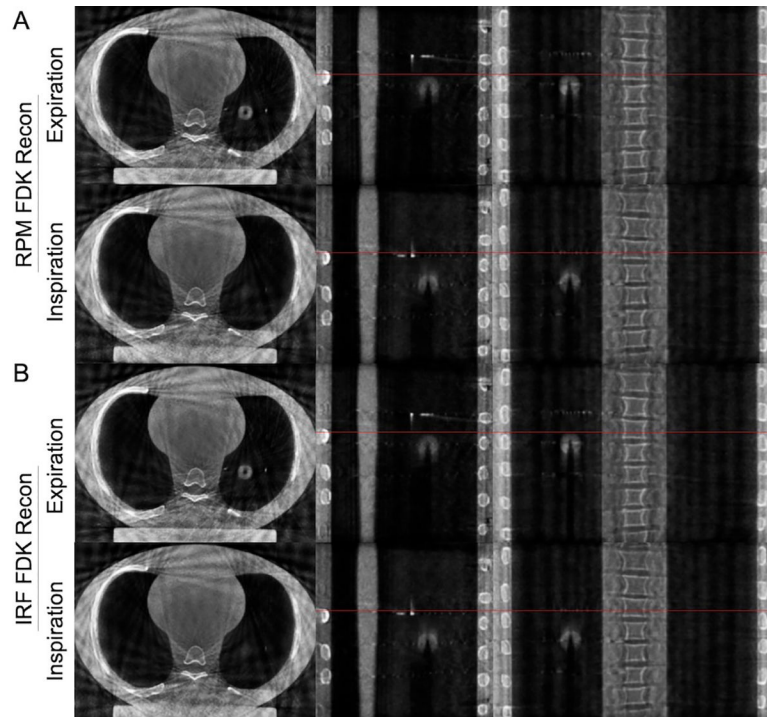


Figure 4. Four-dimensional cone beam computed tomography acquired using the CIRS Dynamic Thorax Motion Phantom and reconstructed using respiratory information provided by the IRF and RPM™ systems. The FDK back-projection algorithm reconstruction using the respiratory phase information provided by either (A) RPM™ or (B) IRF systems provided good qualitative agreement at both inspiration and expiration phases. Red-line = reference line at full-inspiration.

Table 1.

The absolute means and standard deviation differences in amplitude and period between a waveform measured with the IRF and the RPM™ system.

| Mean ± SD | Difference (IRF - RPM™) | | | |
|------------------|-------------------------|--------------|--------------|--------------|
| | Period (s) | Maximum (mm) | Average (mm) | Minimum (mm) |
| RPM Phantom | 0.03 ± 0.21 | 0.22 ± 0.13 | -0.27 ± 0.42 | -0.36 ± 0.26 |
| CIRS Phantom | | | | |
| <i>Low Freq</i> | 0.01 ± 0.14 | 0.12 ± 0.05 | 0.10 ± 0.47 | -0.14 ± 0.03 |
| <i>Med Freq</i> | 0.02 ± 0.05 | -0.30 ± 0.04 | -0.04 ± 0.37 | 0.37 ± 0.05 |
| <i>High Freq</i> | 0.09 ± 0.05 | -0.74 ± 0.04 | -0.01 ± 0.05 | 0.82 ± 0.06 |
| <i>Low Amp</i> | 0.02 ± 0.04 | -0.29 ± 0.03 | -0.05 ± 0.37 | 0.37 ± 0.05 |
| <i>Mid Amp</i> | 0.02 ± 0.04 | -0.73 ± 0.06 | -0.18 ± 0.34 | 0.71 ± 0.06 |
| <i>High Amp</i> | 0.01 ± 0.01 | 0.20 ± 0.05 | 0.52 ± 0.49 | 0.21 ± 0.06 |
| Volunteer 1 | -0.02 ± 0.08 | 0.32 ± 0.54 | -0.09 ± 0.73 | -0.59 ± 0.39 |
| Volunteer 2 | -0.02 ± 0.32 | -0.23 ± 1.16 | 0.71 ± 1.52 | -0.23 ± 1.28 |

SD: standard deviation; IRF: Instant Respiratory Feedback; RPM™: Real-time Position Management™ (Varian Medical Systems); Freq: frequency; Amp: amplitude; Med: medium.

Table 2.Relationships between IRF and the RPMTM systems for both phantoms and human volunteers.

| IRF vs RPM TM | Pearson Correlation | | | | Bland-Altman (cm) | |
|--------------------------|---------------------|-------|----------------|---------|-------------------|--------------|
| | slope | r | r ² | p-value | bias ± SD | CI |
| RPM Phantom | 0.938 | 0.997 | 0.994 | <0.0001 | -0.02 ± 0.04 | -0.11 – 0.06 |
| CIRS Phantom | | | | | | |
| <i>Low Freq</i> | 0.990 | 0.997 | 0.995 | <0.0001 | -0.01 ± 0.05 | -0.09 – 0.11 |
| <i>Med Freq</i> | 1.016 | 0.999 | 0.999 | <0.0001 | -0.01 ± 0.03 | -0.06 – 0.05 |
| <i>High Freq</i> | 1.033 | 0.997 | 0.995 | <0.0001 | -0.02 ± 0.06 | -0.13 – 0.09 |
| <i>Low Amp</i> | 1.017 | 0.999 | 0.999 | <0.0001 | -0.01 ± 0.02 | -0.06 – 0.05 |
| <i>Mid Amp</i> | 1.019 | 0.999 | 0.999 | <0.0001 | -0.02 ± 0.04 | -0.10 – 0.07 |
| <i>High Amp</i> | 1.003 | 0.999 | 0.999 | <0.0001 | 0.05 ± 0.04 | -0.03 – 0.13 |
| Volunteer 1 | 0.962 | 0.996 | 0.991 | <0.0001 | 0.01 ± 0.09 | -0.17 – 0.18 |
| Volunteer 2 | 0.912 | 0.981 | 0.962 | <0.0001 | 0.07 ± 0.15 | -0.23 – 0.37 |

SD: standard deviation; IRF: Instant Respiratory Feedback; RPMTM: Real-time Position ManagementTM (Varian Medical Systems); CI: confidence interval; Freq: frequency; Amp: amplitude; Med: medium.